STRUCTURAL ANALYSIS TECHNOLOGY FOR HIGH-TEMPERATURE DESIGN*

W.L. GREENSTREET

Holifield National Laboratory,
Oak Ridge, Tennessee 37830, U.S.A.

SUMMARY

Results from an ongoing program devoted to development of a verified high-temperature structural design technology are described. This technology embraces design methods and criteria applicable to inelastic behavior of reactor system components under time-varying temperature and load conditions. The major aspects addressed by the program are (1) deformation behavior; (2) failure associated with creep rupture, brittle fracture, fatigue, creep-fatigue interactions, and crack propagation; and (3) the establishment of appropriate design criteria.

This paper discusses information developed in the deformation behavior category, which includes studies of materials behavior; development of mathematical analogs, or constitutive equations, to describe this behavior; and the development and assessment of structural analysis methods. The material considered is type 304 stainless steel, and the temperatures range to 1100°F (593°C).

First, results obtained through uniaxial tests to study elastic-plastic, creep, and relaxation behavior are described. Results from specialized tests for examining various loading history aspects along with combined stress test results are also included. These data were obtained as a part of relatively long-term efforts to provide experimental bases for the development of constitutive equations which realistically model nonlinear hereditary mechanical behavior.

Constitutive equations identified and developed for interim use in design analyses are then discussed. Since the equations were to fill current and near-term needs, existing knowledge in the constitutive equation area, current computational methods and capabilities, and mechanical property data requirements entered into the equation recommendations. In addition, small deformation behavior was assumed to prevail in application, and it was postulated that the total strain tensor could be decomposed into time-independent (elastic and plastic) components and time-dependent (creep) components. Thus, constitutive equations were considered for each type of deformation.

The constitutive equations were incorporated into finite-element computer codes developed under the overall program. Results from two computer codes, a research type and a special-purpose type, for treating plane and axisymmetric structures are compared with experimental data. The latter were obtained from beam and plate specimens tested at 1100°F (593°C) and from a straight-pipe specimen tested at temperatures varying from 800 to 1100°F (427 to 593°C). The beam and plate specimens were simply supported and subjected to concentrated force loadings at the center. Fully reversed cyclic loadings were employed. The straight-pipe specimen was subjected to internal pressure and thermal transient loadings. The maximum temperature was 1100°F (593°C), and the thermal transients were induced by flowing sodium inside the specimen; the combination of pressure and transient loadings produced ratchetting. Generally good agreement between calculated and experimental results was obtained for each specimen type.

In essence, the paper considers the ingredients necessary for predicting relatively high-temperature inelastic deformation behavior of engineering structures and gives some examples. These examples illustrate the utility and acceptability of the computational methods identified and developed for predicting essential features of complex inelastic behavior. Conditions and responses that can be encountered under nuclear reactor service conditions are invoked in the examples.

* Research sponsored by the Energy Research and Development Administration under contract with Union Carbide Corporation.

1. Introduction

The continuing challenge of understanding and predicting inelastic behaviors of metal structures under complex loading conditions has recently been heightened by design requirements imposed by the design of Liquid-Metal Fast Breeder Reactor (LMFBR) components and systems. The relatively high operating temperatures, the very good heat transfer characteristics of the sodium coolant, the long design lifetimes, and the safety, reliability, and operability demands combine to require detailed examinations of inelastic behaviors of the structures involved. The mechanical behaviors of the materials of construction must be understood and the inherent capabilities of these materials utilized to the fullest extent possible commensurate with good practice.

This paper discusses the ingredients associated with inelastic analyses for predicting deformation behaviors and describes the technology currently in use by LMFBR design analysts. These ingredients include mechanical behavior information on the materials of construction, constitutive equations to mathematically describe these behaviors, and certified structural analysis methods and tools.

2. Mechanical Behavior

This discussion is restricted to type 304 stainless steel; the temperatures of interest range up to about 1100°F (593°C). Material from a single reference heat of type 304 stainless steel was used in obtaining all mechanical property and structural test data described in this paper, except for three cases. All specimens were given a full anneal at 2000°F (1093°C) for 30 min.

To illustrate the short-time behavior of the material, stress-strain results from tensile tests at various temperatures and from cyclic loading between fixed strain limits are shown in Figs. 1a and 1b, respectively. The pronounced increase in deformation resistance, or hardening, of this material with increased plastic deformation can be seen in Fig. 1b for two temperature levels. However, hardening and hardening retention are influenced by several factors; accumulated plastic strains increase hardening, whereas hold times at zero stress and high temperature, periods of creep, and periods of relaxation reduce it.

Combined-stress tests of thin-walled cylindrical specimens subjected to axial and torsional loads were used to obtain data on yield surface behavior. The stress corresponding to approximately 10 μin. (25.4 μmm) offset strain was defined as the yield stress in this case. A yield locus obtained at room temperature and subsequent yield curves associated with prestressing along straight-line loading paths are shown for one tubular specimen in Fig. 2a. The subsequent loci correspond to the prestressing points (indicated by the crosses), which are generally outside the corresponding yield loci. The von Mises formulation gives good descriptions of initial yield surfaces as shown; these surfaces move and change in size and shape with plastic deformation.

Figure 2b shows subsequent yield surfaces at various temperatures. To obtain these results, a thin-walled cylindrical specimen was heated to 500°F (260°C) and prestressed to point P shown in the first diagram. Yield loci were then determined at 500°F and sequentially at each of the lower temperatures indicated, except for the first prestressing case. In this case, after the 500°F curve (dashed) was obtained and the temperature was reduced to 350°F (177°C), the specimen was unintentionally loaded to point Q. Hence, the procedure was reinitiated by moving the stress point to near the center of the elastic region and again

heating to 500°F. The two 500°F curves in the first diagram are not markedly different, but the 500°F curves were affected most by subsequent changes in prestressing. The yield curves at the higher temperatures were enclosed by those at the lower temperatures for each of the three prestressing cases (maximum total effective strain of ~0.7%).

Time-dependent behavior of type 304 stainless steel is illustrated by the creep strain vs time results from constant-load constant-temperature tests shown in Fig. 3. Step-load, cyclic-load, and relaxation test results are shown in Fig. 4. Figures 4b and 4c show the cyclic load behavior, where the first half cycle is in tension in one case and in compression in the other.

Combined-stress loading creep behavior was also examined using thin-walled cylindrical specimens that were subjected to axial force and torsional moment loadings. Data obtained by Findley [1] from a 1000-hr, 1100°F (593°C) test in which the axial and torsional stress was 10.63 and 6.11 ksi (73.29 and 42.13 MPa), respectively, are shown in Fig. 5. A constant ratio of the strains with time is seen in Fig. 5a, while Figs. 5b and c depict the axial and torsional responses respectively.

3. Constitutive Equations

Research is continuing to characterize material behaviors and to derive constitutive equations which realistically describe the complex hereditary nonlinear mechanical behaviors exhibited. To meet existing design needs, constitutive equations were identified and developed for interim use. The resultant recommendations were based on combined considerations of existing knowledge in the constitutive equation area, current computational methods and capabilities, and mechanical property data requirements.

Small deformation behavior was assumed to prevail in application, and it was postulated that the total strain tensor could be decomposed into time-independent (elastic and plastic) and time-dependent (creep) components. Thus, constitutive equations were considered for each type of deformation. Classical kinematic hardening theory [2, 3, 4] was recommended [5, 6] for use in describing elastic-plastic behaviors of stainless steels. This theory provides acceptable representations of essential features of the observed behavior; its use is compatible with computational methods currently employed and with the existing materials data base. The classical theory was modified along lines described by Prager [7] to account for temperature effects, and auxiliary rules were provided to account for, in an approximate way, additional influences of deformation history on subsequent deformation response.

An equation-of-state type formulation was adopted [5, 6] for use in expressing creep strain rates (both primary and secondary) in terms of applied stresses and other variables. This selection represented a logical choice for near-term use in view of current data for use in design analyses and of the lack of relevant information on creep behavior. Through comparison with experimental data, the strain-hardening rule [8, 9] was selected to represent responses under changing stress conditions. However, since the usual strain-hardening procedure does not apply in cases of stress reversals, auxiliary rules were also provided.

To complete the examination of elements for multiaxial creep formulations, several expressions for representing creep strains under constant uniaxial stress and temperature conditions were studied. Candidate equations are shown in Fig. 3b. The first employs two exponential terms to describe primary creep strains, while the other two contain single-term representations. The first equation was selected for design use since it gives good fits to

experimental data at both short and long times. However, the second equation was used to obtain calculated responses described later in this paper.

Comparisons between computed and measured results for the uniaxial case are given in Fig. 4. The predictions in the cyclic creep and relaxation cases (Figs. 4b through 4d) were made on the basis of the single-exponential-term creep equation and data from a group of uniaxial, constant-load creep tests on specimens taken from the same plate of material. The overall agreement is good for the conditions examined. Differences between predicted and measured results stem, at least in part, from lack of agreement in uniaxial test results and from a less than adequate representation, given by the equation selected, of the very steep portion of the uniaxial creep response at the stress levels and very short times of interest.

Calculated and measured results for the combined stress case (Figs. 5b and c) show reasonable agreement.

4. Analysis of Inelastic Structural Response

Structural analysis methods capable of incorporating the constitutive equations and treating geometries and loadings of interest complete the complement of tools needed. To indicate accuracies of results obtained in the analysis of structures, a simply supported, center-loaded circular plate (CP4) was considered. The plate was 20.75 in. (0.527 m) in outside diameter and 0.5 in. (12.7 mm) thick and was loaded by a concentrated force applied through a boss at the center and supported on a 20.0-in. (0.508-m) diameter circle. The test temperature was 1100°F; deflection control was employed, with maximum center deflections being ±0.11 in. (±2.79 mm).

CREEP-PLAST [10] a special-purpose finite-element computer code which was developed under the overall program was used in the structural analysis. This code treats two-dimensional (plane and axisymmetric) structures, employs 3-node triangular elements (2 degrees of freedom at each node) and uniaxial bar elements, and incorporates the recommended constitutive equations and auxiliary calculational procedures. In the analysis, a symmetry section of one-half of the plate was represented by a mesh of 748 axisymmetric revolved triangular elements, giving 928 degrees of freedom. Bilinear representations of stress-strain response were based on cyclic curves for a strain range of 0.4%; the tenth cycle representation was used for all plastic loadings subsequent to the first.

The loading history in terms of center deflection vs time is shown in Fig. 6a for plate specimen CP4. Key points on the diagram are numbered for reference in the other plots of the figure. The measured and predicted load vs center deflection behavior for "instantaneous" load changes from points 1 to 2, 3 to 4, and 5 to 6 are shown in Fig. 6b. The agreement is reasonably good, with the calculated maximum load being somewhat greater than the measured value for each deflection change segment.

The predicted and measured loads during the two hold periods at maximum deflection are shown in Fig. 6c, that is, for the hold (relaxation) periods from 2 to 3 and from 4 to 5. The calculated loads are in much better agreement at the ends of the hold periods than at the beginnings. The overall discrepancies reflect inadequacies in uniaxial creep response representation, as mentioned above. Finally, comparisons of results for the ten short-time cycles (6 to 7 in Fig. 6a) imposed after the second period of relaxation are shown in the load-deflection plot of Fig. 6d, where the curves are plotted from the deflection at zero load. The deformation resistance of the material was less than predicted, giving larger loads under

L 3/2+

positive deflection portions of the cycles than measured. However, the shakedown prediction was good.

Similar agreement was obtained for a simply supported rectangular beam loaded at the center and tested in the deflection control mode. The agreement for load-control situations, although reasonable, is generally not as good, largely because the results are more sensitive to discrepancies in stress-strain response representations. Very good agreement was obtained between predicted and measured results from a test in which a pipe specimen [11] was subjected to complex thermal and mechanical loadings to simulate nuclear reactor service conditions.

5. Conclusions

The results given indicate the state of the art of inelastic structural analysis methodology that is available for general use by design analysts. Despite needs for additional research and development work, essential features of inelastic behaviors of structures under complex time-varying loading conditions can be predicted with reasonable accuracy, giving rational bases for design guidance and performance assessments.

Acknowledgments

My sincere appreciation is extended to the following persons for information contained in this paper: to J. M. Corum and J. A. Clinard for structural analysis and test data; to K. C. Liu and C. E. Pugh for constitutive equation development information; and to R. W. Swindeman for mechanical properties data.

References

[1] FINDLEY, W. N., "Multiaxial Creep Studies," High-Temperature Structural Design Methods for LMFBR Components Quart. Progr. Rep. for Period Ending June 30, 1972, ORNL-TM-3917, pp. 10–25.

[2] PRAGER, W., "The Theory of Plasticity: A Survey of Recent Achievements (James Clayton Lecture," Proc. Inst. Mech. Eng. 169, 41–57 (1955).

[3] SHIELD, R. T., and ZIEGLER, H., "On Prager's Hardening Rule," Z. Ang. Math. Phys. IXA, 260–276 (1958).

[4] ZIEGLER, H., "A Modification of Prager's Hardening Rule," Quart. Appl. Math. 17, 55–65 (1959).

[5] PUGH, C. E., et al., "Currently Recommended Constitutive Equations for Inelastic Analysis of FFTF Components," ORNL-TM-3602 (September 1972).

[6] CORUM, J. M., et al., "Interim Guidelines for Detailed Inelastic Analysis of High-Temperature Reactor System Components," ORNL-5014 (December 1974).

[7] PRAGER, W., "Non-Isothermal Plastic Deformation," Proc. Koninklijke Nederlandsche Akademie van Wetenschappen 61(3B), 176–182 (1958).

[8] ROBOTNOV, Yu N., Creep Problems in Structural Members, pp. 206–207, American-Elsevier Publishing Co., Inc., New York, 1969.

[9] ODQVIST, F. K. G., "Non-Linear Solid Mechanics–Past, Present, and Future," Proc. Twelfth Int. Conf. on Appl. Mech., Stanford University, Aug. 26–31, 1968, pp. 77–99, Springer-Verlag, New York, 1969.

[10] CLINARD, J. A. and CROWELL, J. S., "ORNL User's Manual for CREEP-PLAST Computer Program," ORNL-TM-4062 (November 1973).

[11] CORUM, J. M., and SARTORY, W. K., Elastic-Plastic Creep Analysis of Thermal Ratchetting in Straight Pipe and Comparisons with Test Results, ASME Paper No. 73-WA/PVP-4, 1973.

L 3/2*

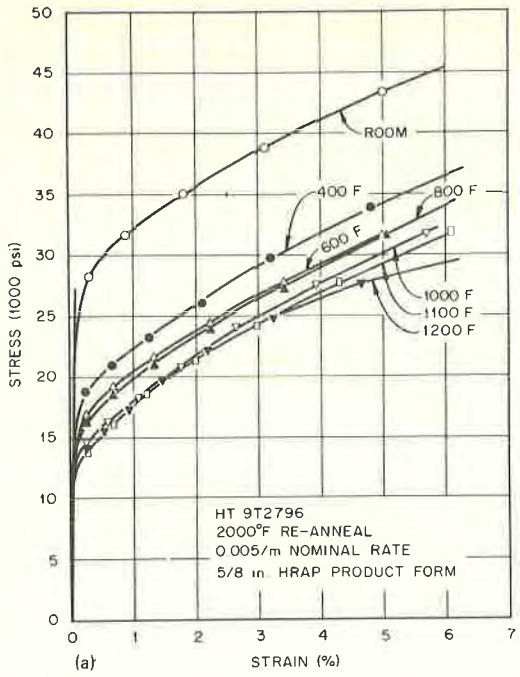

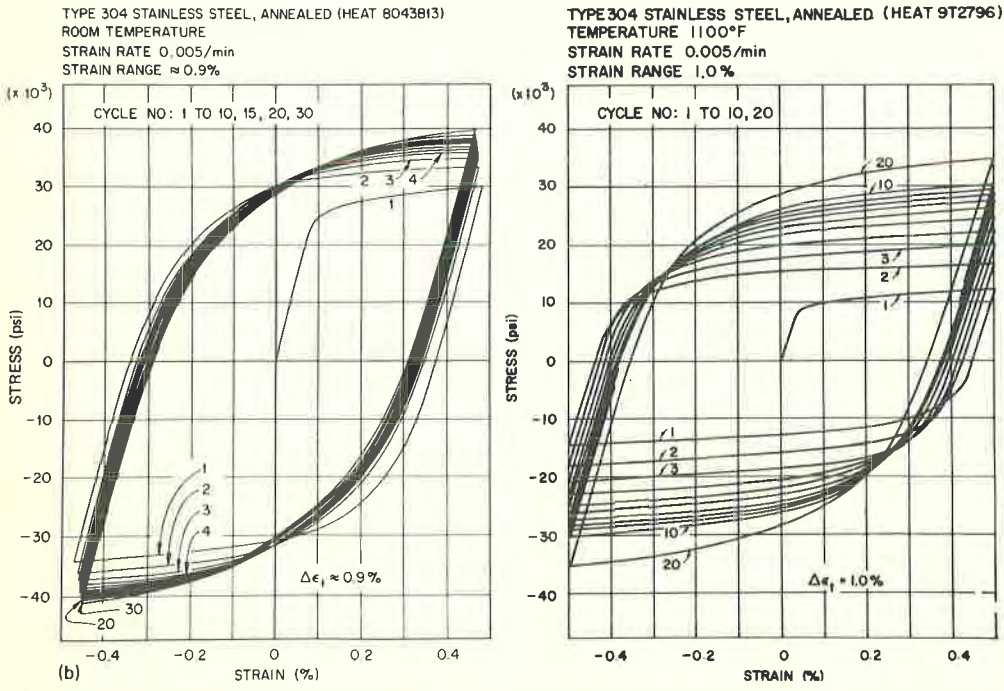

Fig. 1. Stress-strain behavior of an annealed type 304 stainless steel. (a) Monotonic initial loading; (b) typical cyclic loading. (1 ksi = 6.895 MPa)

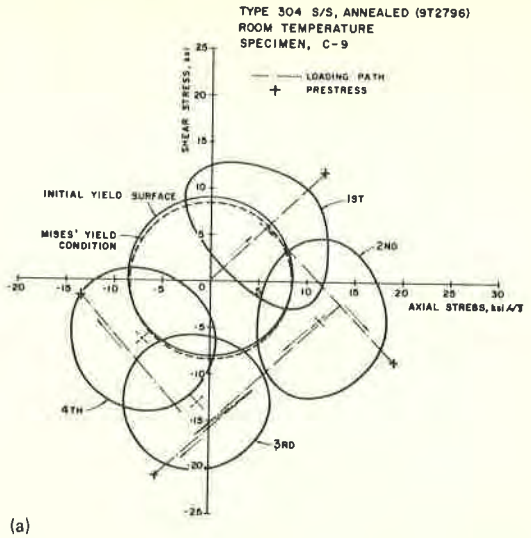

(a)

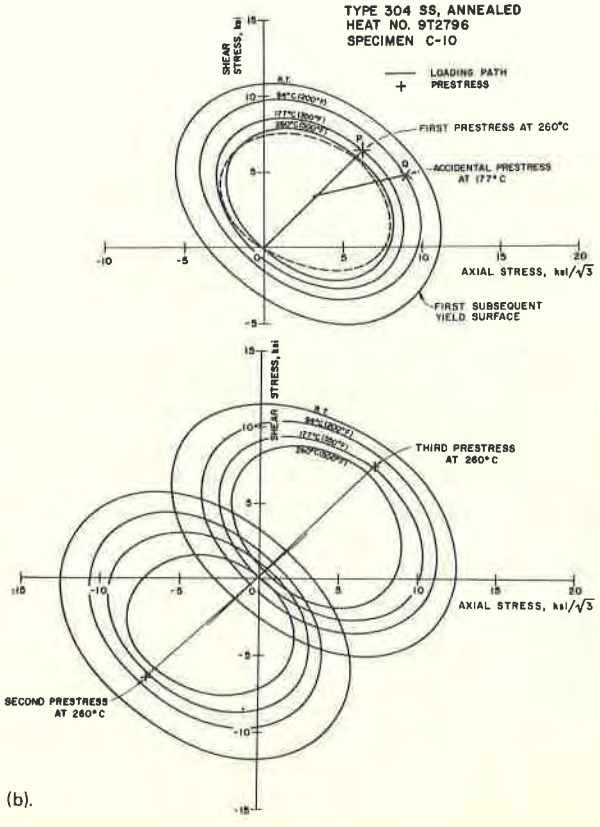

(b).

Fig. 2. Yield surface behavior for type 304 stainless steel. (a) Initial and subsequent yield surfaces at room temperature; (b) subsequent yield surfaces at temperatures to 500°F (260°C). (1 ksi = 6.895 MPa)

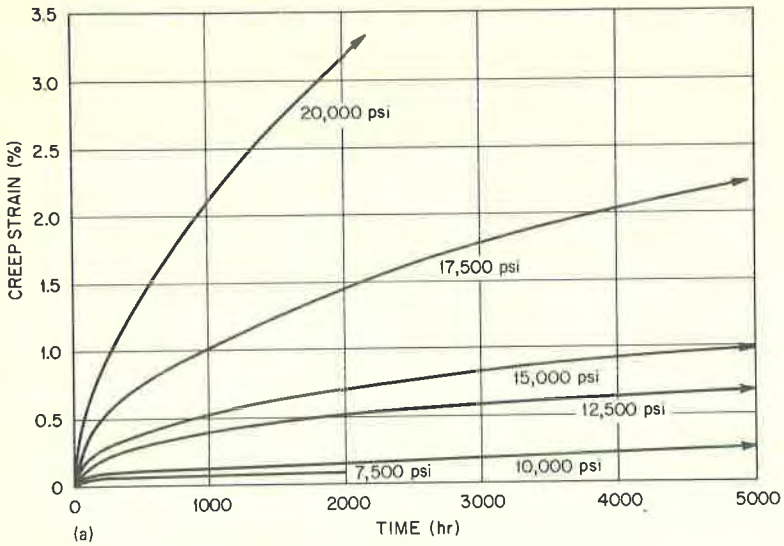

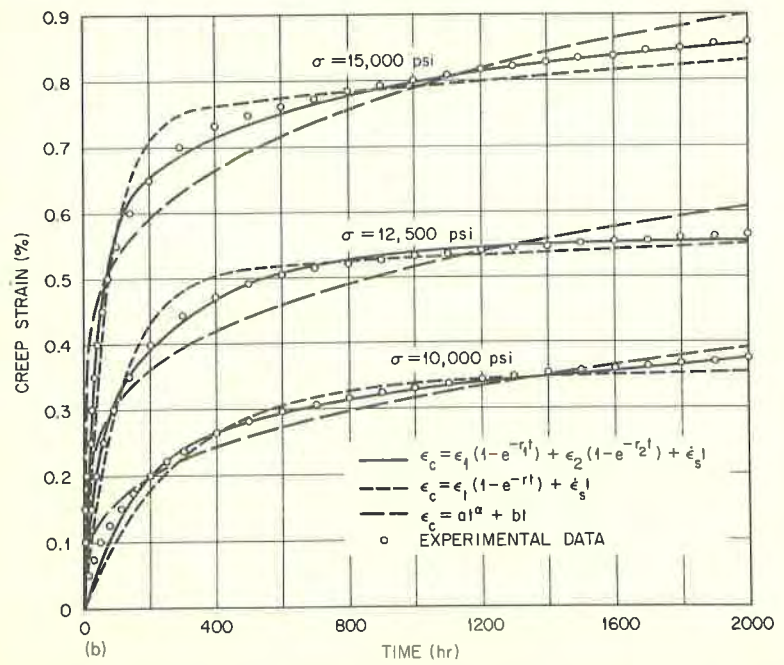

Fig. 3. Creep curves for an annealed type 304 stainless steel. (a) Typical constant-load curves; (b) creep response representations [1200°F (649°C)]. (1 ksi = 6.895 MPa)

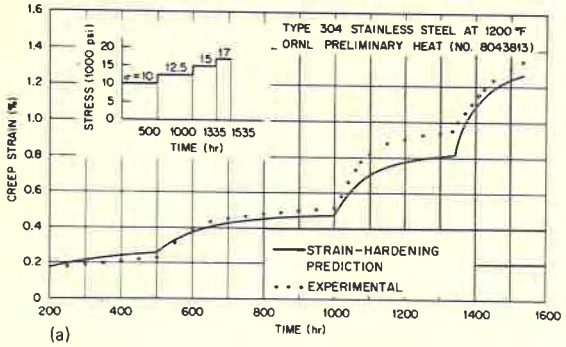

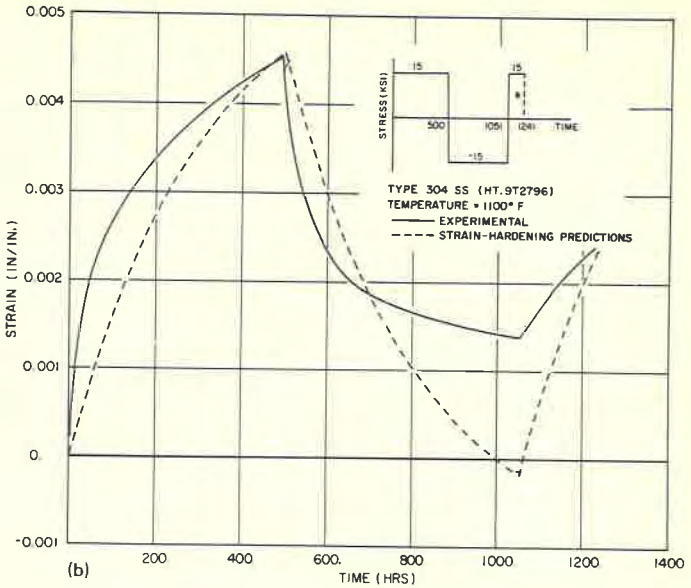

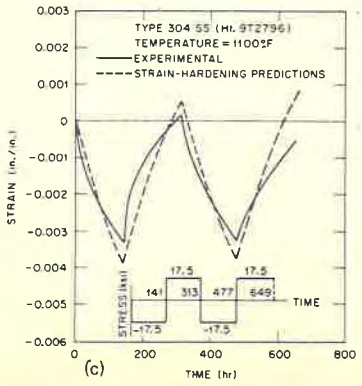

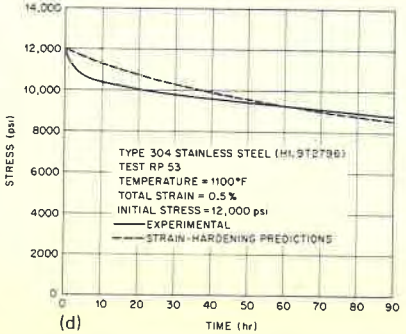

Fig. 4. Time-dependent behavior of annealed type 304 stainless steel at 1100°F (593°C). (a) Step-loading creep test results; (b) cyclic-loading creep test results; (c) cyclic-loading creep test results; (d) relaxation response for 0.5% strain. (1 ksi = 6.895 MPa)

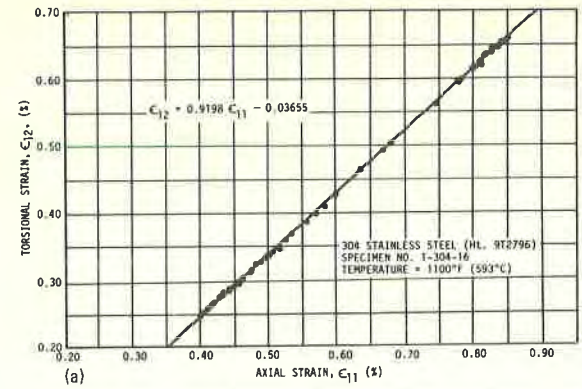

(a)

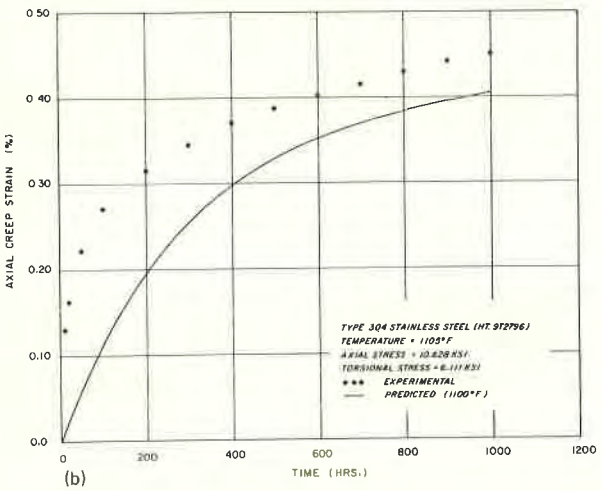

(b)

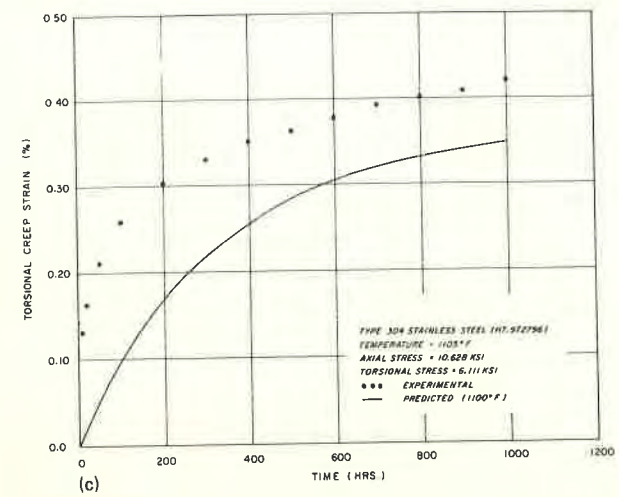

(c)

Fig. 5. Combined-stress creep test results for type 304 stainless steel at 1100°F (593°C). (a) Measured torsional strain vs axial strain (σ = 10.63 ksi, τ = 6.11 ksi); (b) axial creep strain vs time; (c) torsional creep strain vs time. (1 ksi = 6.895 MPa).

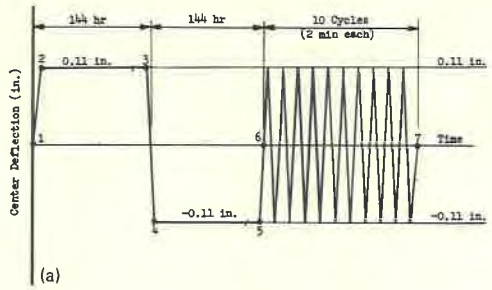

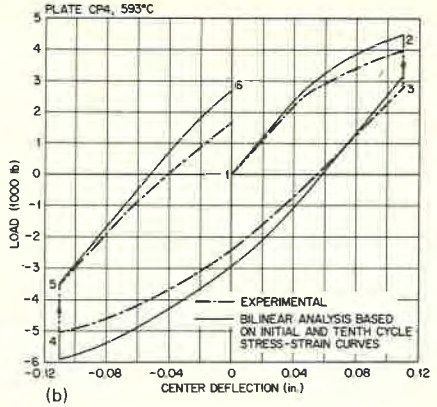

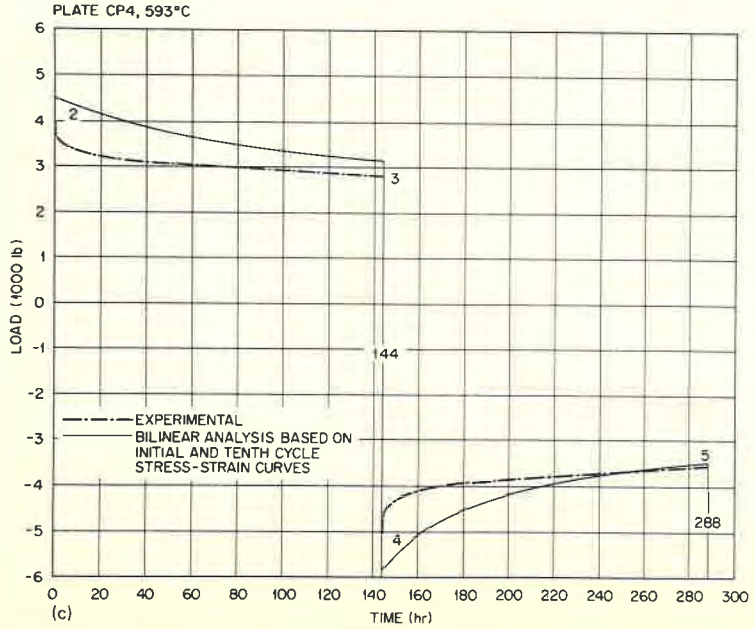

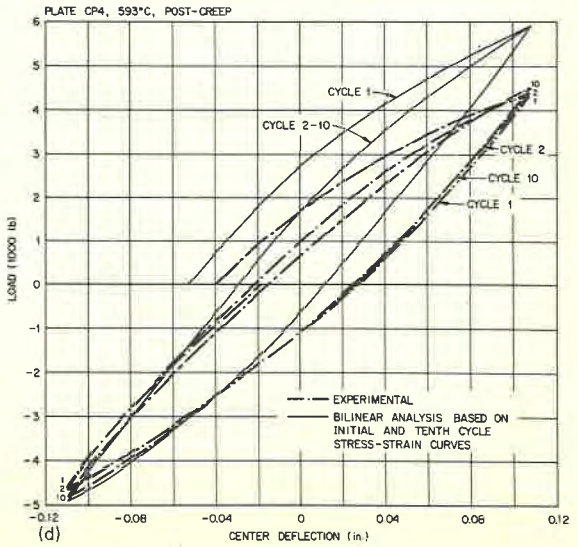

Fig. 6. Results from deflection-controlled tests on simply supported plate (CP4) at 1100°F (593°C). (a) Loading history; (b) behavior during deflection changes; (c) load relaxation vs time; (d) behavior during 10 short-time postrelaxation cyclic loadings. (1 ksi = 6.895 MPa)

L 3/2*